GEOPHYSICAL RESEARCH LETTERS, VOL. 21, NO. 21, PAGES 2295-2298, OCTOBER 15, 1994

Impact of increased CO_2 on simulated ENSO-like phenomena

Thomas R. Knutson and Syukuro Manabe

Geophysical Fluid Dynamics Laboratory, Princeton, New Jersey

Abstract. The impact of a CO_2-induced global warming on ENSO-like fluctuations in a global coupled ocean-atmosphere GCM is analyzed using two multi-century experiments. In the $4xCO_2$ experiment, CO_2 increases by a factor of four in the first 140 years and then remains constant at $4xCO_2$ for another 360 years; in the control experiment, CO_2 remains constant at $1xCO_2$ for 1000 years. The standard deviation of tropical Pacific SST fluctuations (7°N-7°S, 173°E-120°W; 2 to 15 year timescales) is 24% lower in the $4xCO_2$ experiment than in the control experiment; for the model's Southern Oscillation Index, a 19% decrease occurs, whereas for central tropical Pacific rainfall, a 3% increase occurs. An important feature of the control simulation is the internally generated modulation of variability on a multi-century timescale, which is comparable in magnitude to the changes occurring with $4xCO_2$. We conclude that despite an order 5 K warming of the tropical Pacific, and order 50% increase in time-mean atmospheric water vapor under $4xCO_2$ conditions, ENSO-like SST fluctuations in the coupled model do not intensify, but rather decrease slightly in amplitude.

Introduction

How would the magnitude of El Niño/Southern Oscillation events change in response to CO_2-induced global warming? One can speculate that during ENSO episodes in a CO_2-warmed climate, the much larger amounts of atmospheric moisture present would allow for enhanced moisture convergence and condensational heating anomalies, which could induce stronger surface wind anomalies. Through such a mechanism, the strength of the windstress feedback onto the ocean (per degree SST anomaly) could be substantially increased, possibly leading to an increase in the magnitude of ENSO events. In this report, we investigate such a possibility using multi-century simulations of a global coupled ocean-atmosphere general circulation model (GCM).

Meehl et al. (1993) and S. Tett (Hadley Centre, manuscript submitted to *J. Clim.*, 1994) have made preliminary analyses of the impact of increased CO_2 on ENSO-like phenomena in coupled ocean-atmosphere GCMs. Meehl et al. compared results obtained from a 15-year integration period with doubled CO_2 and a simulation with the normal CO_2 concentration ($1xCO_2$). Tett compared results from 75-year simulations during which CO_2 was either increasing at 1% per year compounded or constant at $1xCO_2$. However, in the present study, we will show that substantial internally generated modulation of the ENSO-like phenomena occurs in our coupled model on a multi-century timescale. Moreover, several studies of historical and paleoclimatic records (e.g., Michaelsen, 1987; Enfield and Cid S., 1990; Diaz and Markgraf, 1992; Dunbar and Cole, 1993) show evidence for variations in both the frequency and amplitude of ENSO on multi-decadal to century timescales.

These results suggest that *multi-century* integrations are useful for more reliably determining the impact of increased CO_2 on ENSO-like phenomena in coupled models. Therefore, in this report we analyze control and CO_2 perturbation experiments of length 1000 and 500 years, respectively, using a large perturbation ($4xCO_2$) to enhance any CO_2-induced signal in the model.

Paper number 94GL02152

Description of Model and Filters

The coupled ocean-atmosphere model and experimental design used here are described in Manabe and Stouffer (1994), and references therein. Briefly, the atmospheric component is a global nine-level GCM, with horizontal distributions of variables represented in both spectral (rhomboidal truncation at zonal wavenumber 15) and gridpoint (7.5° longitude by 4.5° latitude computational grid) domains. The ocean component is a global 12-level gridpoint GCM with 3.75° longitude by 4.5° latitude resolution. The model has interactive cloud and seasonally varying solar insolation. An adjustment of the heat and water fluxes at the atmosphere-ocean interface is used to prevent spurious climate drift from a realistic initial condition (Manabe and Stouffer 1994). The adjustments vary with season and geography, but not from year to year. Since they are independent of the anomalies of temperature and salinity at the ocean surface, they neither damp nor amplify the anomalies. Furthermore, Lau et al. (1992) found ENSO-like fluctuations similar to those described here using a similar model but with no heat flux adjustment, indicating that the ENSO-like phenomena appear in the absence of heat flux adjustment.

The three primary filters used in our analysis have response > 0.9 at periods of: i) > 24 months (lowpass); ii) > 50 years (very lowpass); and iii) 24 months to approximately 15 years (bandpass). These are designed following Hamming (1977, Ch. 7), and have 0.5 response at 21 months and 25 years. The 2-15 year timescale is chosen to correspond approximately to the timescale of the model's ENSO-like phenomenon. The basic conclusions of our study are not altered if a narrower (e.g., 2-4 years) or broader (e.g., >2 year) timescale is used.

Overview of the Model's ENSO-like Phenomena

Here we present a brief overview of the model's ENSO-like phenomenon in the control experiment. Lau et al. (1992) present an extensive analysis of ENSO-like phenomena in a GFDL coupled ocean-atmosphere GCM similar to that used here, but without a seasonal cycle or interactive cloud.

Figure 1(a) shows the lagged correlation between sea-surface temperature (SST) over the central tropical Pacific and sea-level pressure (SLP) at each model gridpoint. SLP anomalies are out-of-phase between the Indonesia region and the southeast Pacific, similar to the classical Southern Oscillation pattern of Berlage and others (e.g. Julian and Chervin 1978).

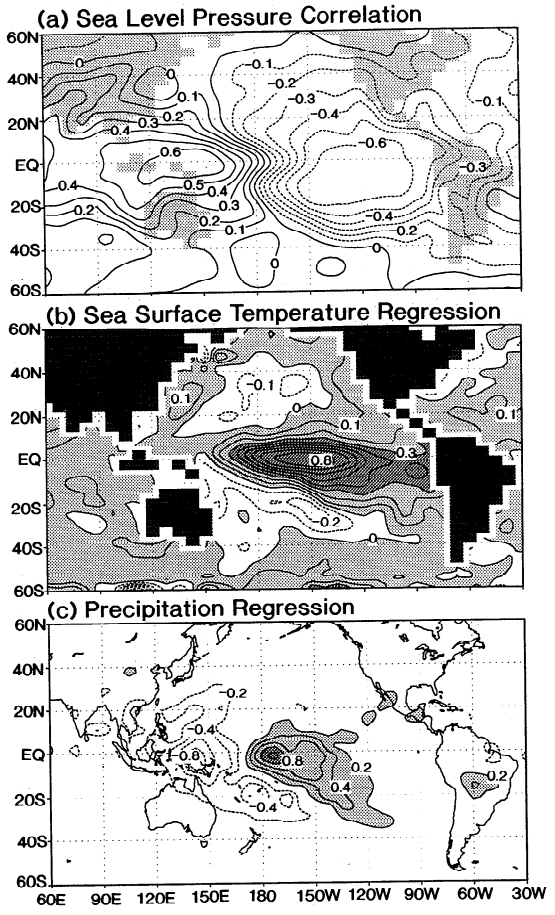

Figure 1. a) Lagged correlation map of sea level pressure (SLP) vs. SST (7°N-7°S, 172.5°E-120°W). b) Lagged regression map of SST vs. the negative of the model "Southern Oscillation Index" (SOI), defined as the SLP at 11°S, 127.5°W minus that at 2°S, 142.5°E; contour: 0.1 K/mb. c) As in (b), but for precipitation vs SOI; contour: 0.2 mm/day/mb. Based on lowpass (>24 month) filtered data from years 6-195 of the control experiment, with SST and precipitation lagging SLP by three months.

Figure 1(b) shows a map of the lagged regression coefficients for the model's "Southern Oscillation Index" (SOI) vs SST at every gridpoint. This map indicates that when the surface pressure gradient defined by the SOI is near its minimum, accompanied by decreased easterly surface winds over the tropical Pacific (e.g., Lau et al. 1992), a broad area of positive SST anomalies occurs over the tropical Pacific. The positive tropical SST anomalies are flanked by negative SST anomalies in the extratropics of both hemispheres. The SST regression pattern in Figure 1(b) resembles the Mature Phase composite of Rasmusson and Carpenter (1982), although the model's most pronounced interannual SST variability is too confined to the central Pacific compared to observations. The lagged regression pattern for precipitation (vs. the model SOI) in Figure 1(c) shows that warm SST episodes are accompanied by increased precipitation over the central tropical Pacific and suppressed precipitation over Indonesia. The model's precipitation anomalies resemble the observed patterns of Ropelewski and Halpert (1987) for the Pacific basin, although differences are apparent in more remote regions.

Our model's SST (SOI) fluctuations, with a typical amplitude of order 1°C (1 mb) or less, are weaker than those of the observed ENSO (e.g. Rasmusson and Carpenter, 1982; Neelin et al. 1994). This is a problem common to several other simulations of ENSO-like phenomena using low resolution ocean models (Lau et al., 1992; Meehl et al., 1993; Tett,1994; Neelin et al., 1992). The amplitude appears to increase to more realistic values when a much higher resolution model of the tropical Pacific ocean is used (e.g., Philander et al. 1992).

The timescale of the real ENSO has been about 2-10 years over the past century (Trenberth, 1976), although as noted previously the timescale has apparently fluctuated over the past several centuries. We estimate, from analyses of variance and coherence spectra for SST and the model SOI, that the model phenomenon has a broad timescale of about 2 to 15 years. The model's ENSO-like phenomenon does not exhibit pronounced seasonal cycle phase-locking, as occurs for the real ENSO (Rasmusson and Carpenter, 1982). However, we note that some coupled GCMs do not necessarily require a seasonal cycle to produce ENSO-like variability (e.g., Lau et al., 1992; Philander et al., 1992), although the seasonal cycle apparently regulates the initiation and progression of ENSO-like anomalies in the low-resolution coupled GCM of Meehl (1990).

Despite its very coarse resolution, our model, which has a velocity gridpoint located on the equator, appears to at least crudely resolve both the slow, eastward propagating ENSO timescale equatorial thermocline variations and the faster, higher frequency uncoupled Kevin and Rossby modes identified in the much higher resolution simulation of Philander et al. (1992). For example, upper ocean (300 meter) heat content anomalies propagate eastward along the equator and westward (more slowly) at about 11°N and 11°S on both long (>24 months) and short (<18 month) timescales (not shown). The phase speeds of the high-frequency features are similar to those in Philander et al. (1992), although the amplitude is reduced by about 50%. Equatorial Pacific SST anomalies typically propagate westward in our model, particularly on 2-4 year timescales, although eastward propagation occasionally occurs. Our model's ENSO-like phenomenon exhibits behavior corresponding to a regime of the "mixed SST/ocean dynamics mode" of Neelin et al. (1994 and references therein). The apparently important role of SST propagation, coupled with the relatively small impact of fluctuations in the vertical temperature gradient on the heat budget of the top 50-meter ocean layer (i.e., $\overline{w}T_z'$ in Lau et al., 1992), suggests that the model phenomenon is more closely related to Neelin's "SST mode" with a lesser role for subsurface ocean dynamics than occurs with the higher resolution model of Philander et al. (1992).

The differences between our simulation (see also Lau et al. 1992) and that of Philander et al. (1992) indicate that our ocean model's low resolution and high eddy viscosity have an important impact on the model's ENSO-like phenomenon and tropical Pacific ocean climatology. Nevertheless, the considerable resemblance between the ENSO-like phenomena in our model and both the observed ENSO and the high-resolution simulation of Philander et al. suggests that useful preliminary information about the impact of increased CO_2 on ENSO can be obtained using the low-resolution model.

Impact of Increased CO_2

The impact of increased CO_2 on the model's ENSO-like phenomena is now considered by comparing the control experiment with a 4xCO_2 experiment. In the latter, CO_2 increases at 1%/year (compounded) for 140 years and then remains at four

times the normal concentration ($4xCO_2$) for 360 more years. The large-scale patterns of the model's Southern Oscillation and related SST and precipitation anomaly fields from the $4xCO_2$ experiment (not shown) are very similar to those from the control experiment (Figure 1). Therefore, we will use indices of area-averaged SST, precipitation, and the model's Southern Oscillation to determine whether changes in the amplitude of the ENSO-like phenomenon occur in response to CO_2 increases in the model. The region of largest positive precipitation anomalies shifts eastward by about one gridpoint (7.5° longitude) in the $4xCO_2$ experiment vs. the control experiment; to account for this shift, the precipitation index is constructed using a large domain (11°N-11°S, 173°E-113°W).

Figure 2 shows the SST index from the $4xCO_2$ and control experiments. In the $4xCO_2$ experiment, SSTs rise rapidly during the buildup of CO_2 (years 1-140), followed by a 360-year period of more gradual warming, as the climate continues adjusting to the constant $4xCO_2$ forcing. By years 401-500, tropical SSTs increase by about 4.2 K (5.3 K) in the western (eastern) Pacific, resulting in a 20% decrease in the zonal SST gradient (not shown). The model's ENSO-like phenomenon is evident throughout the $4xCO_2$ experiment as distinct interannual departures of SST from the slowly changing basic state.

The temporal evolutions of the standard deviations for both 2-15 year filtered SST and the model SOI (Figure 3a, b) indicate decreased variability after the initial CO_2 buildup period of the $4xCO_2$ experiment. During the entire 1000-year control experiment, the standard deviation for 100-year segments of SST never reaches levels as low as those for the final 200 years of the $4xCO_2$ experiment. The standard deviation from years 161-480 of the $4xCO_2$ experiment (0.21 K) is 24% less than that from years 21-980 of the control run (0.28 K). Similarly, for the SOI, a 19% decrease occurs in the $4xCO_2$ experiment.

Another important feature of Figure 3 is the internally generated fluctuation in variability of SST and the SOI that occurs between different 100-year segments of the control experiment. These fluctuations are of comparable magnitude to the differences between the $4xCO_2$ and control experiments. A comparison of the variance spectra for detrended SST timeseries from the $4xCO_2$ and 1000-year control experiments (not shown) indicates that the decreases in variance in the $4xCO_2$ experiment are statistically significant (non-overlapping 95% confidence intervals) for 21% of the spectral estimates in the 2-15 year band. Nevertheless, the practical importance of these decreases remains unclear, particularly

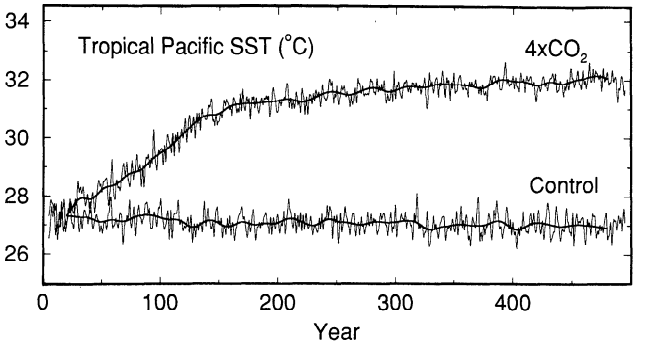

Figure 2. SST (7°N-7°S, 173°E-120°W) from the $4xCO_2$ and control experiments. Shown are low-pass (>24 month) and very low-pass (> 50 year) filtered timeseries from each experiment.

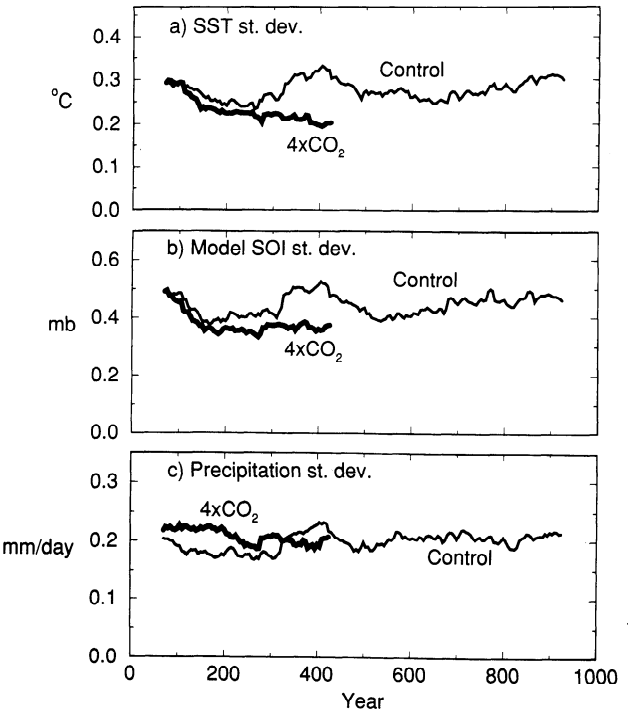

Figure 3. Standard deviations of overlapping 100-year segments of bandpass (2-15 year) filtered anomalies from the $4xCO_2$ and control experiments. a) SST (7°N-7°S, 173°E- 120°W) in °C; b) SOI (see Figure 1(b) caption) in mb; and c) precipitation (11°N-11°S, 173°E-113°W) in mm/day.

since the magnitude of the apparent CO_2-induced change is not substantially larger than the internally generated fluctuations in amplitude occurring in the model on a multi-century timescale.

The standard deviation of the tropical Pacific precipitation index (e.g., Figure 3c) is 3% larger in years 161-480 of the $4xCO_2$ experiment, compared to years 21-980 of the control. Moreover, the precipitation anomaly per Kelvin SST anomaly (as estimated by linear regression) increases by over 23% in the $4xCO_2$ experiment. We note that the globally averaged standard deviation of monthly mean precipitation increases by over 20% by the end of the $4xCO_2$ experiment, reminiscent of the studies of Rind et al. (1989) and Meehl and Washington (1993). Thus, the 3% increase for the 2-15 year fluctuations of the tropical Pacific precipitation index is unusually small--in comparison to the typical CO_2-induced response of precipitation variability in the model--owing to the decreased amplitude of ENSO-like SST fluctuations in the $4xCO_2$ experiment.

The 23% increase in precipitation anomalies (per K SST anomaly) mentioned above, is associated with the very large (i.e. 45%) increase in the time-mean vertically integrated water vapor content of air in the $4xCO_2$ experiment. The increased moisture allows for greater anomalous moisture convergence over the central equatorial Pacific during ENSO warm episodes and thus enhances the precipitation anomaly (per K). However, the strength of the atmosphere-ocean coupling in the model, as estimated by the surface zonal wind anomaly (2°N-2°S, 150°E-113°W) per degree SST anomaly, increases by a much smaller fraction (0.99 m/s/K vs. 1.12 m/s/K, or 12%), than the condensation heating (precipitation) per K (i.e. 23%). Analysis of the atmospheric heat budget indicates that the enhanced condensation heating anomaly (per K) is balanced primarily by en-

hanced cooling by anomalous rising motion ($-w'\partial\bar{\theta}/\partial z$). However, anomalous rising motions (w') intensify mainly in the upper troposphere due to deeper penetration of convection. Moreover, about 60% of the enhancement of vertically integrated dynamical cooling can be attributed to a slight increase in the time-mean vertical gradient of potential temperature ($\partial\bar{\theta}/\partial z$) alone. This increased static stability is an effect of moist convection, which keeps the vertical lapse of temperature close to the moist adiabatic rate, making $\partial\bar{\theta}/\partial z$ larger in a warmer atmosphere. This lapse rate mechanism helps explain why the anomalous zonal overturning circulation, and thus the surface zonal wind anomaly per K, does not increase in proportion to the increase of condensation heating (per K) in the model.

Enhanced evaporative damping (per K) of SST anomalies and a ~20% reduction of the time-mean zonal SST gradient in the equatorial Pacific are important factors contributing to the net weakening of the ENSO-like SST fluctuations in the $4xCO_2$ experiment despite the slightly stronger surface zonal wind anomalies (per K) mentioned above. This assessment is based on analysis of the ocean surface layer heat budget following Lau et al. (1992).

Discussion and Conclusions

ENSO-like phenomena similar to those in the control experiment continue to occur throughout the $4xCO_2$ experiment. Although a modest decrease in the variability of SST and SOI anomalies occurs in the $4xCO_2$ experiment, the magnitude of this decrease is not markedly greater than the internally generated fluctuations in variability that occur between different 100-year segments of the control experiment. The lack of a CO_2-induced intensification of ENSO-like SST fluctuations is consistent with Meehl et al. (1993) and Tett (1994).

Our results indicate the importance of using model integrations of sufficient length to adequately sample the internally generated variation in the coupled system when examining external influences on ENSO-timescale variability. For example, we can obtain estimates of the CO_2-induced change in variability of from -10 to -37% for SST and from -3 to -31% for the SOI, simply by choosing a different 100-year period from the control simulation as the "baseline."

The resolution/diffusivity of the ocean component of our model has a notable impact on the amplitude and structure of the model's ENSO-like variability (Philander et al. 1992). However, the use of a much higher resolution ocean model for extensive climate simulations was precluded for our study by the large computer requirements of such models. Nevertheless, we believe that the mechanisms we have identified that prevent an increase in the amplitude of the ENSO-like fluctuations (i.e., increased atmospheric static stability, decreased time-mean zonal SST gradient, and enhanced evaporative damping of SST anomalies), will not be greatly sensitive to model resolution.

We conclude that while the possibility of significant CO_2-induced increases in the amplitude of ENSO SST fluctuations cannot be ruled out (given current model limitations) evidence for such changes has not been found in the present study, despite the greatly enhanced flux of moisture to the atmosphere and the much larger moisture content of air in the $4xCO_2$ climate. An intriguing result from our analysis, worthy of further study, is the variation in the amplitude of the ENSO-like phenomenon on a centennial timescale, due solely to internal processes in the coupled model.

Acknowledgments. We thank R. Stouffer for providing the results from the successful long-term integration of the coupled model; N.-C. Lau, S.G.H. Philander, I. Held, C. Lindberg, D. Neelin and others for useful discussions; three anonymous reviewers for helpful comments; and J.D. Mahlman for whole-hearted support.

References

Diaz, H.F., and V. Markgraf (Eds.), *El Niño: Historical and Paleoclimatic Aspects of the Southern Oscillation*, 476 pp., Cambridge Univ. Press, Cambridge, 1992.

Dunbar, R.B., and J.E. Cole, Coral records of ocean-atmosphere variability, *NOAA Climate and Global Change Program Special Report No. 10*, 38 pp., Univ. Corp. Atm. Res., 1993.

Enfield, D.B. and L. Cid S., Low-frequency changes in El Niño-Southern Oscillation, *J. Clim., 4*, 1137-1146, 1991.

Hamming, R.W., *Digital Filters*, 226 pp., Prentice-Hall, Inc., Englewood Cliffs, NJ, 1977.

Julian, P.R. and R.M. Chervin, A study of the Southern Oscillation and Walker Circulation phenomenon, *Mon. Wea. Rev., 106*, 1433-1451, 1978.

Lau, N.-C., S.G.H. Philander, and M. J. Nath, Simulation of ENSO-like phenomena with a low-resolution coupled GCM of the global ocean and atmosphere, *J. Clim., 5*, 284-307, 1992.

Manabe, S. and R.J. Stouffer, Multiple century response of a coupled ocean-atmosphere model to an increase of atmospheric carbon dioxide, *J. Clim., 7*, 5-28, 1994.

Meehl, G. A., Seasonal cycle forcing of El Niño-Southern Oscillation in a global, coupled ocean-atmosphere GCM, *J. Clim., 3*, 72-98, 1990.

Meehl, G.A., G.W. Branstator, and W.M. Washington, Tropical Pacific interannual variability and CO_2 climate change, *J. Clim., 6*, 42-63, 1993.

Meehl, G.A., and W.M. Washington, South Asian summer monsoon variability in a model with doubled atmospheric carbon dioxide concentration, *Science, 260*, 1101-1104, 1993.

Michaelsen, J., Long-period fluctuations in El Niño amplitude and frequency reconstructed from tree rings, in *Aspects of climate variability in the Pacific and the western Americas*, edited by D.H. Peterson. pp. 69-74, *Geophys. Mono. 55*, AGU, 1989.

Neelin, J.D., et al., Tropical air-sea interaction in general circulation models, *Clim. Dyn., 7*, 73-104, 1992.

Neelin, J.D., M. Latif, and F.-F. Jin, Dynamics of coupled ocean-atmosphere models: the tropical problem, *Annu. Rev. Fluid Mech., 26*, 617-659, 1994.

Philander, S.G.H., R.C. Pacanowski, N.-C. Lau, and M.J. Nath, Simulation of ENSO with a global atmospheric GCM coupled to a high-resolution, tropical Pacific ocean GCM, *J. Clim., 5*, 308-329, 1992.

Rasmusson, E.M. and T.H. Carpenter, Variations in tropical sea surface temperature and surface wind fields associated with the Southern Oscillation/El Niño, *Mon. Wea. Rev., 110*, 354-384, 1982.

Rind, D., R. Goldberg and R. Ruedy, Change in climate variability in the 21st century, *Climatic Change, 14*, 5-37, 1989.

Ropelewski, C.F. and M.S. Halpert, Global and regional scale precipitation patterns associated with the El Niño/Southern Oscillation, *Mon. Wea. Rev., 115*, 1606-1626, 1987.

Trenberth, K.E., Spatial and temporal variations of the Southern Oscillation, *Quart. J. R. Met. Soc., 102*, 639-653, 1976.

T.R. Knutson and S. Manabe, Geophysical Fluid Dynamics Laboratory/NOAA, P.O. Box 308, Princeton, NJ 08542. (e-mail: tk@gfdl.gov)

(Received February 23, 1994; revised June 17, 1994; accepted August 1, 1994.)